

Article

Endowing Ferroelectric Properties of Tetragonal Lysozyme Crystals through C₆₀ Doping

Renbin Zhou , Xuejiao Liu, Weihong Guo and Dachuan Yin * 

Key Laboratory for Space Bioscience and Biotechnology, School of Life Sciences, Northwestern Polytechnical University, 127 Youyixi Road, Xi'an 710072, China; zhourb@nwpu.edu.cn (R.Z.); 2023264375@mail.nwpu.edu.cn (X.L.); gwh@nwpu.edu.cn (W.G.)

* Correspondence: yindc@nwpu.edu.cn

Abstract: The inherent nonpolarity of tetragonal lysozyme crystals excludes a ferroelectricity response. Herein, we present a demonstration of achieving measurable ferroelectricity in tetragonal lysozyme crystals through C₆₀ doping. Ferroelectric characterizations revealed that C₆₀-doped tetragonal lysozyme crystals exhibited typical characteristic ferroelectric hysteresis loops. Crystallographic structural analysis suggested that C₆₀ doping may induce a reduction in the overall symmetry of tetragonal Lys@C₆₀, leading to the observed ferroelectricity response. Moreover, the introduction of C₆₀ facilitates efficient electron transport inside the crystal and influences the polarization of Lys@C₆₀, further contributing to the observed ferroelectricity response. This work verifies that C₆₀ doping can serve as a simple strategy to bestow novel ferroelectric properties to non-ferroelectric lysozyme crystals, potentially rendering them suitable for biocompatible and biodegradable application in implantable and wearable bioelectronics.

Keywords: protein crystals; C₆₀; ferroelectricity



Citation: Zhou, R.; Liu, X.; Guo, W.; Yin, D. Endowing Ferroelectric Properties of Tetragonal Lysozyme Crystals through C₆₀ Doping. *Crystals* **2024**, *14*, 339. <https://doi.org/10.3390/cryst14040339>

Academic Editors: Blaine Mooers and Jolanta Prywer

Received: 30 December 2023

Revised: 19 January 2024

Accepted: 27 March 2024

Published: 1 April 2024



Copyright: © 2024 by the authors. Licensee MDPI, Basel, Switzerland. This article is an open access article distributed under the terms and conditions of the Creative Commons Attribution (CC BY) license (<https://creativecommons.org/licenses/by/4.0/>).

1. Introduction

Crystalline materials exhibit a variety of unique physical properties, such as piezoelectricity, pyroelectricity, and ferroelectricity, which can convert external stimuli (such as mechanical stress, heat, electricity, and light) into electrical and optical signals, making them ideal for biomedical applications [1,2]. Piezoelectricity, observed only in crystals with a non-centrosymmetric structure, involves the generation of electricity under stress [3]. Pyroelectricity, a subset of piezoelectricity, exhibits spontaneous polarization to generate electrical energy under temperature fluctuations [4]. Ferroelectricity is characterized by switchable spontaneous polarization, where the direction of electric dipoles can be re-orientated under a sufficiently high electric field [5,6]. The piezoelectricity, pyroelectricity, and ferroelectricity of crystalline materials are governed by their symmetry. Among the 32 point groups of the crystal, 21 lack non-centrosymmetry, and 20 of them exhibit piezoelectric effects. Within these crystal forms, 10 piezoelectric point groups are polarizable (1, 2, m, mm2, 3, 3m, 4, 4mm, 6 and 6mm), potentially indicating ferroelectric characteristics [7,8]. However, most crystalline materials are non-ferroelectric, restricting the development and application of ferroelectric materials [9]. Strategies that can feasibly transform non-ferroelectric materials into ferroelectric ones will extend their applications in energy storage and conversion.

We hypothesize that doping may endow non-ferroelectric materials with ferroelectric properties. Fullerene (C₆₀) exhibits unique electric properties, and previous research has widely documented that C₆₀ doping can induce a new emergent high charge conductance in electrically insulating protein assemblies [10]. Therefore, C₆₀ doping may achieve the non-ferroelectric to ferroelectric transformation. Currently, research on the ferroelectricity of proteins is limited to fibril protein types [11–13], with elastin extensively studied in this context [14,15]. However, there is a relative lack of research on the ferroelectric properties

of nonfibrillar proteins [16,17]. Lysozyme, a widely studied globular protein, has a non-centrosymmetric structure, satisfying the basic premise of piezoelectricity [8,18], while the most common tetragonal form of lysozyme crystals (P422) are nonpolar and lack ferroelectricity, making them an ideal model to check whether C_{60} doping can transform non-ferroelectric P422 tetragonal lysozyme crystals into ferroelectric ones.

In this study, we demonstrated that C_{60} doping can endow ferroelectric properties to tetragonal lysozyme crystals (P422), presenting a feasible strategy to prepare ferroelectric materials for bio-applications. Results from a conductive atomic force microscope (c-AFM) and switching-spectroscopy piezoresponse force microscopy (SS-PFM) revealed a significant increase in electrical conductance and ferroelectricity in P422 tetragonal lysozyme crystals after C_{60} doping, indicating that C_{60} doping can indeed serve as a feasible strategy to impart novel ferroelectric properties to non-ferroelectric protein crystals, extending the applications of protein crystals in electrical fields.

2. Methods

2.1. Preparation of $Lys@C_{60}$ Tetragonal Crystals

Initially, a lysozyme- C_{60} complex solution (hereafter abbreviated as $Lys@C_{60}$) was prepared using an ultrasonic method [19,20]. Specifically, 10 mg of lysozyme was mixed with 10 μ g of C_{60} powder in a sodium acetate buffer (100 mM, pH 4.8). Subsequently, the mixed solution underwent ultrasonication on ice with a tip (50 mW, 2 s work, 6 s pause). The resulting solution was then centrifuged at 4 °C with 8000 rpm, and the supernatant was collected for further use.

To generate tetragonal crystals, a protein crystallization method was employed [21,22]. Briefly, an 80 mg/mL $Lys@C_{60}$ solution was blended with crystallization precipitants (40 mg/mL NaCl). For the assessment of ferroelectric properties, $Lys@C_{60}$ tetragonal crystals were grown on ITO-coated glass slides. Once the crystals had formed, the crystallization solution was discarded, and the crystals were washed three times with crystallization precipitants to eliminate any uncrystallized protein. Finally, the washed crystals were cross-linked using 1% glutaraldehyde to enhance the stability. Simultaneously, tetragonal lysozyme crystals were prepared using the same crystallization methods mentioned above for comparative analysis.

2.2. Characterization of $Lys@C_{60}$ Tetragonal Crystals

Thermogravimetric analysis: The thermal stability of $Lys@C_{60}$ crystals and lysozyme crystals was assessed using the thermogravimetric analyzer. A 5 mg freeze-dried sample underwent heating to 700 °C at a rate of 5 °C/min, and the corresponding data were recorded.

Structural analysis: The $Lys@C_{60}$ crystal, suitable for X-ray single crystal diffraction, was obtained using the hanging-drop method at 293 K. A 2 μ L drop, consisting of a 1:1 *v/v* mixture of 80 mg/mL $Lys@C_{60}$ solution in 100 mM sodium acetate buffer (pH 4.8) and a reservoir solution of 40 mg/mL NaCl in 100 mM sodium acetate buffer (pH 4.8), was employed. After two days of incubations, the obtained crystal was flash-frozen by transferring it to an antifreeze solution containing 20% glycerol in the reservoir solution. Subsequently, the diffraction data were collected using a household diffractometer at 100 K with diffraction parameters set as follows: X-ray wavelength of 1.54179 Å, diffraction distance of 150 mm, exposure time of 5 min/photo, and a rotation angle of 1°. The acquired diffraction data were processed with HKL 2000, and then scaled with CCP4. The structure was solved by rigid-body refinement with phenix.refine in Phenix software (version 1.11) [23]. The protein structure refinement was finished with phenix.refine and REFMAC5 in the CCP4 suite. The structure rebuilding was performed by COOT with sigma-A weighted $2|Fo| - |Fc|$ and $|Fo| - |Fc|$ electron density maps [24,25].

2.3. Conductive Performance of $Lys@C_{60}$ Tetragonal Crystal

To directly measure the conductive properties of $Lys@C_{60}$, a conductive atomic force microscope (c-AFM) was employed [26]. The ITO- $Lys@C_{60}$ electrode was securely affixed

to the sample stage using silver tape. The sample's conductivity was assessed using a CONTSPT probe, and the resulting current was directly recorded through a preamplifier with a gain ranging from 10^9 to 10^{11} V/A. The c-AFM spectrum was obtained by applying a voltage of 5 V to the sample and subsequently scanning the sample surface.

The resistance of Lys@C₆₀ was quantified through electrochemical impedance spectroscopy (EIS) using an electrochemical workstation. The experimental setup included a nickel foam–Lys@C₆₀ crystal as the working electrode, a saturated calomel electrode as the reference electrode, a platinum electrode as the counter electrode, and a 1 × PBS electrolyte. The bias voltage was maintained at 0 V throughout the experiment. The voltage of the current–time (I–T) curve was set to 0.5 V, and the scan time extended over a period of 30 min.

2.4. Ferroelectric Performance of Lys@C₆₀ Tetragonal Crystals

To investigate the ferroelectric performance of Lys@C₆₀ crystals and lysozyme crystals, switching spectroscopy piezoresponse force microscopy (SS-PFM) was employed [27]. The experimental setup involved fixing the ITO–Lys@C₆₀ electrode or ITO–Lys electrode on the sample stage using silver tape. The tip's oscillation frequency and amplitude were configured at 1 KHz and 50 nm, respectively. The alternating voltage (VAC) frequency was set at 10 KHz, and the direct voltage (VDC) range spanned from –5 V to 5 V. The scanning protocol involved an initial forward scan, followed by a reverse scan, and the results were recorded for subsequent analysis.

3. Result

3.1. Characterization of Lys@C₆₀ Crystal

The physical properties of protein crystals, such as ferroelectricity, are governed by their crystallographic symmetry [28]. Various lysozyme crystal forms can be obtained using different crystallization conditions [29]. In this work, tetragonal Lys@C₆₀ crystals were obtained as expected. As shown in Figure 1a, the optical microscopy image illustrates the tetragonal form of Lys@C₆₀ crystals on the ITO electrode. It is noteworthy that within the tetragonal crystal, two available crystals forms (Point Group 422 and Point Group 4) exist. The symmetry constraints play a pivotal role in determining the ferroelectric properties of these crystals [30]. Theoretically, Point Group 4 crystals are expected to be polar and exhibit ferroelectric properties, whereas chiral Point Group 422 crystals are not (Figure S1). The investigation into whether the C₆₀ doping alters the symmetry is crucial before study the ferroelectric properties. Therefore, to accurately determine the point group symmetry of Lys@C₆₀ crystals, X-ray single-crystal diffraction was employed for crystal structure determination. As depicted in Figure 1b, the highest diffraction resolution achieved for the Lys@C₆₀ crystal is 2.1 Å. Subsequent structural analysis revealed that the obtained Lys@C₆₀ crystal belongs to the same P₄₃2₁2 point group as the original lysozyme crystal. Detailed structural data are listed in Table S1. The diffraction spectra of lysozyme crystal are presented in Figure S2. After structural alignment (Figure 1c), it is evident that the structure of the Lys@C₆₀ crystal remains consistent with that of the original lysozyme crystal. These results demonstrate that the doping of C₆₀ does not affect the conformation and point group symmetry of lysozyme crystals.

3.2. Enhancing Stability of Lys@C₆₀ Crystals for Ferroelectric Property Measurement

Protein crystals exhibit soft and brittle characteristics due to their higher water content, varying from 17.4% to 47.2% in different crystal forms [31]. To preserve their inherent structure and prevent cracking and degradation during the measurement of ferroelectric properties, the mechanical properties of proteins can be improved through chemical cross-linking [32]. In this study, Lys@C₆₀ crystals underwent cross-linking with glutaraldehyde to enhance their stability. The cross-linked Lys@C₆₀ crystals displayed significantly improved stability, maintaining their morphology at room temperature without alterations in space group symmetry and structure (Figure 1a–c). To further assess the stability of cross-

linked Lys@C₆₀ crystals, thermogravimetric analysis (TGA) was conducted. Figure 1d illustrates that the weight loss of Lys@C₆₀ crystals occurs in three distinct stages. The first stage (0 °C–100 °C) involves the evaporation of 7% bound water in the Lys@C₆₀ crystal. During the second stage (100 °C–200 °C), the mass of Lys@C₆₀ crystal remains essentially constant, indicating that glutaraldehyde cross-linking significantly enhances the thermal stability of the crystal, enabling it to withstand temperatures up to 200 °C. The third stage (200 °C–700 °C) involves pyrolysis, resulting in an 80% mass loss for Lys@C₆₀ crystals. The TGA results for lysozyme crystals are essentially consistent with those of Lys@C₆₀ crystals, suggesting that the doping of C₆₀ does not compromise the thermal stability of lysozyme crystals. Consequently, the stability of Lys@C₆₀ crystals is substantially improved after cross-linking treatment, meeting the characterization requirements for evaluating ferroelectric performance.

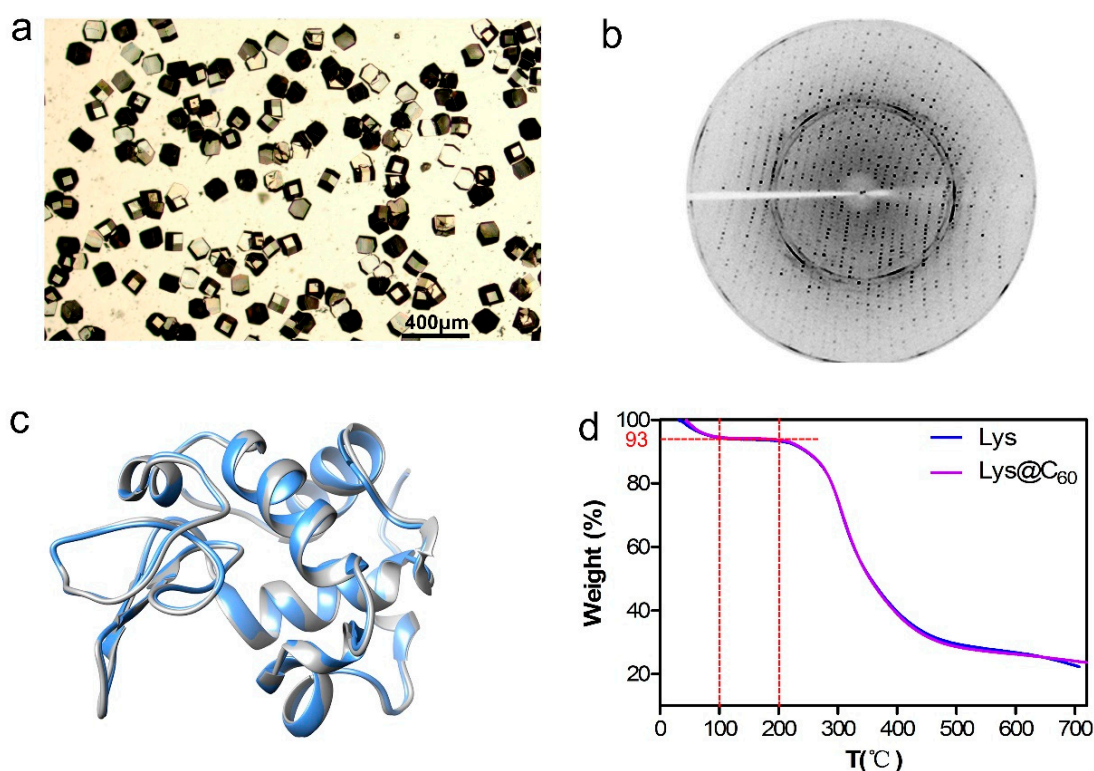


Figure 1. Characterization of Lys@C₆₀ crystals. (a) optical image of Lys@C₆₀ tetragonal crystals; (b) the diffraction pattern of Lys@C₆₀ crystal; (c) the structure alignment of Lys@C₆₀ (blue color) and lysozyme (gray color); (d) the TGA analysis of Lys@C₆₀ and lysozyme crystals.

3.3. Ferroelectric Evaluation of Lys@C₆₀ Crystals

As previously stated, lysozyme crystals with the P₄₃2₁2 point group exhibit non-ferroelectric properties. In order to investigate whether C₆₀ doping will endow ferroelectricity to P₄₃2₁2 point group lysozyme crystals, the ferroelectric performance of Lys@C₆₀ crystals is evaluated with piezoresponse force microscopy (PFM). PFM has evolved as a powerful tool for measuring the conductivity and ferroelectric properties of materials at the nanoscale. Based on the inverse piezoelectric effect, a specified voltage is applied to the piezoelectric sample through the cantilever beam of the atomic force conductive microscope, inducing sample deformation. During scanning of the sample surface by the atomic force microscope probe, the deformation induced by the sample's electric field can be detected. Additionally, utilizing the polar scanning method, the piezoelectric force microscope can measure the ferroelectric properties of the sample [33]. If the sample possesses ferroelectric properties, the spontaneous polarization of the sample will change with variations in the applied voltage, allowing the detection of the sample's ferroelectric properties.

In our study, a piezoelectric force microscope was employed to apply a voltage of 5 V to the Lys@C₆₀ crystal through a conductive probe, scanning the sample surface with an area of ($5 \times 5 \mu\text{m}^2$). When a crystal is polarized, the polarity can be detected through scanning. Figure 2a,b illustrate the absence of polarity (ferroelectric domain) in the lysozyme crystal, consistent with the theory that the P₄₃2₁2 lysozyme crystal cannot spontaneously polarize. In contrast, the Lys@C₆₀ crystal, as anticipated, exhibited clear ferroelectric domains and domain walls in different directions in its amplitude diagram (Figure 2c). Moreover, the phase diagram (Figure 2d) revealed domain inversion, indicating that through C₆₀ doping, Lys@C₆₀ crystals can indeed exhibit spontaneous polarization. Therefore, Lys@C₆₀ crystals may possess ferroelectric properties, offering promising prospects for further applications.

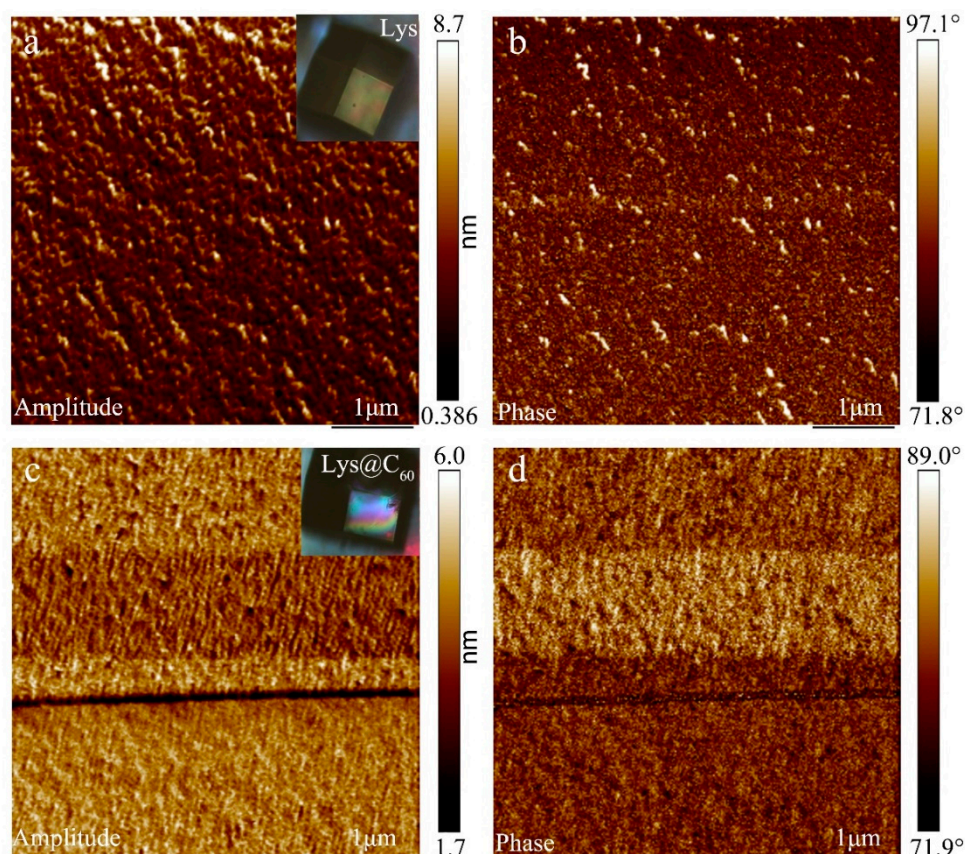


Figure 2. The ferroelectricity of lysozyme and Lys@C₆₀ crystals. (a) The amplitude of lysozyme crystals; (b) the phase of lysozyme crystals; (c) the amplitude of Lys@C₆₀ crystals; (d) the phase of Lys@C₆₀ crystals.

To provide further confirmation of ferroelectricity, the characteristic hysteresis loop of Lys@C₆₀ crystals was measured using switching-spectroscopy piezoresponse force microscopy (SS-PFM). In the presence of ferroelectricity, the spontaneous polarization undergoes reversal under the applied field, resulting in a distinctive butterfly loop pattern. As illustrated in Figure 3a,b, the control group exhibits negligible butterfly curves and hysteresis loops for lysozyme crystals, aligning with the theoretical expectation that the P₄₃2₁2 crystal form of lysozyme lacks a ferroelectric effect. Contrastingly, as anticipated, the switching phase loop (Figure 3c) and butterfly-shaped amplitude (Figure 3d) for Lys@C₆₀ clearly indicate its ferroelectric nature. Notably, the characteristic hysteresis loops display asymmetry, suggesting the presence of internal bias within the Lys@C₆₀ crystal. This internal bias is hypothesized to arise from the bound water within Lys@C₆₀ (hydration layer). Due to its strongly bound nature, this water is resistant to the switching direction. As corroborated by the thermogravimetric results (Figure 1d), approximately 7% bound water exists within Lys@C₆₀ crystals. Therefore, these findings demonstrate that C₆₀

doping can indeed bestow ferroelectric properties of the originally non-ferroelectric $P4_32_12$ lysozyme crystal.

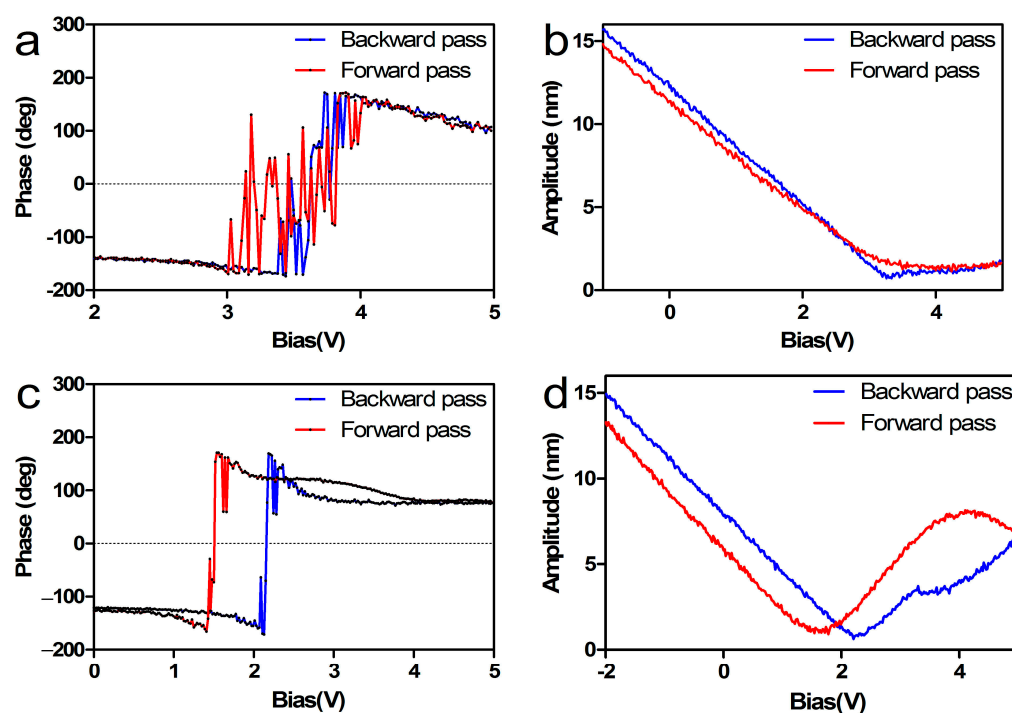


Figure 3. The ferroelectricity of lysozyme and Lys@C_{60} crystals. (a) The switching phase loop of lysozyme crystals; (b) the butterfly shape amplitude of lysozyme crystals; (c) the switching phase loop of Lys@C_{60} crystals; (d) the butterfly shape amplitude of Lys@C_{60} crystals.

Encouraged by its ferroelectric properties, Lys@C_{60} may be used as potential biocompatibility implantable devices in biomedical applications. The cytotoxicity of Lys@C_{60} in HEK 293 cells was assessed using the CCK-8 method. As depicted in Figure S3, the excellent biocompatibility of Lys@C_{60} was observed in HEK 293 cells treated with varying concentrations (0.1 mM, 0.2 mM, 0.3 mM, and 0.4 mM), indicating the biosafety of Lys@C_{60} for biomedical applications.

3.4. Explanation of Observed Ferroelectricity in Lys@C_{60} Crystals

3.4.1. Lowering Symmetry by C_{60} Doping

The emergent ferroelectricity of Lys@C_{60} crystals can be explained through two possible mechanisms. One is that doping C_{60} may lower the entire symmetry of the Lys@C_{60} crystal hybrid. Although the X-ray crystallography data determine the $P4_32_12$ point group of Lys@C_{60} crystals, the absence of a C_{60} electron map suggests a disordered distribution of C_{60} within the lysozyme crystals (Figure 1c). This disordered C_{60} arrangement may lower the overall symmetry of the Lys@C_{60} crystal hybrid allowing for switchable spontaneous polarization and resulting in ferroelectricity.

3.4.2. Influence on Polarization by Emerging Conductivity

Another explanation involves C_{60} doping influencing the polarization of lysozyme crystals by its emerging conductivity. Assembling C_{60} into electrically insulating protein crystals has been documented to alter the charge distribution and achieve high conductance protein- C_{60} hybrid [10]. Thus, the influence of C_{60} on the polarization of Lys@C_{60} crystals can be detected by the conductivity. To assess the conductive performance of Lys@C_{60} crystals, conductive force microscopy (c-AFM) was employed. As shown in Figure 4a, lysozyme crystals alone exhibit electrical insulation with zero current, whereas, after C_{60} doping, Lys@C_{60} crystals display a weak current of 200 pA, indicating electrical conductivity. This

observation is further supported by the current diagram from the conductive atomic force microscope. Again, the lysozyme crystal surface is electrical insulating (Figure 4b), while most of the Lys@C₆₀ crystal surface is not conductive, linear areas with higher conductivity are dispersed across the surface, and the measured current represents an average. In the most conductive areas, currents can reach approximately 1000 pA (Figure 4c). The disorder distribution of C₆₀ within the lysozyme crystal, as indicated by the absence of an electron map in the Lys@C₆₀ crystal during structural analysis (Figure 1c), explains this phenomenon. Therefore, the introduction of C₆₀ facilitates efficient electron transport inside the crystal, contributing to the observed ferroelectricity response.

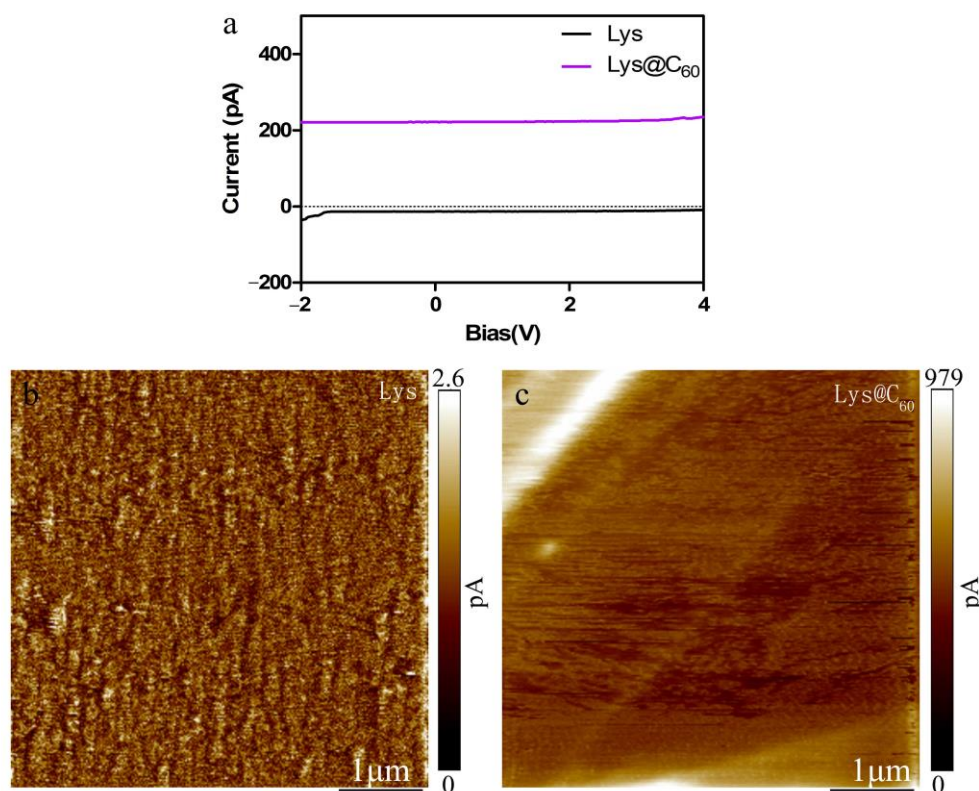


Figure 4. The electrical properties of Lys@C₆₀ crystals. (a) The I-V curve of Lys@C₆₀ crystals; (b) the c-AFM map of lysozyme crystals; (c) the c-AFM map of Lys@C₆₀ crystals.

The assessment of C₆₀ doping enhancing the conductivity of Lys@C₆₀ crystals is also indirectly supported by measuring the impedance of Lys@C₆₀ crystals grown on nickel foam (Figure S4). As depicted in the provided Figure S5, Lys@C₆₀ crystals exhibit a significant reduction in resistance compared to lysozyme crystals alone. It is crucial to emphasize that the measured impedance primarily reflects the resistance of the nickel foam. In reality, both Lys@C₆₀ crystals and lysozyme crystals contribute to an overall increase in the resistance of the nickel foam. However, Lys@C₆₀ crystals demonstrate less resistance compared to lysozyme crystals, indirectly suggesting the improved conductivity of Lys@C₆₀. This additional evidence strengthens the conclusion of the enhanced conductive performance of Lys@C₆₀ crystals resulting from C₆₀ doping. In summary, the enhanced conductivity induced by C₆₀ doping is a key factor in the newfound ferroelectric properties of Lys@C₆₀ crystals.

4. Discussion

Ferroelectric materials, with their reorientable polarization, show great promise for energy storage and generation, particularly in implantable or wearable biomedical applications [34]. Protein crystals, owing to their unique structure symmetry and biodegradability, are considered ideal bio-ferroelectric materials. However, their inherent electrical insula-

tion and fragile nature impede their application in electrical fields. This study aimed to develop methods to improve the stability and electrical properties of protein crystals for electro-mechanical applications.

The primary challenge in studying the electrical properties of protein crystals lies in their poor stability. Unlike other inorganic materials, the direct preparation of protein crystals into electrodes for electrical measurement is challenging. To overcome this issue, cross-linking with glutaraldehyde was employed, significantly enhancing the stability and mechanical properties of lysozyme crystals. Remarkably, even when exposed to temperatures as high as 200 °C, the lysozyme crystal structure remained intact (Figure 1d). Another significant challenge is the direct electroding of lysozyme crystals for electric-mechanical measurements. In this study, we successfully carried out the electroding of lysozyme crystals onto conductive substrates (ITO film and nickel foam) to enable electrochemical performance characterization (see Figure S2). And the conductive substrate did not affect Lys@C₆₀ crystal preparation, allowing their use as electrodes for testing electrical properties.

Additionally, considering the poor electrical conductivity of protein crystals, efforts were made to enhance lysozyme crystal conductivity through C₆₀ doping. The combined results from direct measurements of conductivity through atomic force microscopy and indirect measurements of resistance and current on nickel foam demonstrate that C₆₀ doping does improve the conductivity of lysozyme crystals. The observed I-V curve of Lys@C₆₀ crystals does not exhibit ohmic characteristics (Figure 4a), indicating that the doping content of C₆₀ is low. Under low C₆₀ doping conditions, a tunnel barrier is present in the crystal channel. The mechanism underlying this conductivity improvement is attributed to the disorderly arrangement of C₆₀ within the lysozyme crystal, effectively acting as p-type doping and forming pairs of holes and electrons. Under the influence of an electric field, the movement of carriers within the crystal results in the generation of an electric current. C₆₀ doping enhancing the conductivity of lysozyme crystals pave the way for new applications of protein crystals in the field of bioelectronics.

Surprisingly, C₆₀ doping introduced intriguing ferroelectricity to P422 tetragonal lysozyme crystals. The characteristic ferroelectric hysteresis loops of Lys@C₆₀ crystals were detected with SS-PFM (Figure 3), despite the theoretical expectation that P4₃2₁2 tetragonal lysozyme crystals lack the ability for spontaneous polarization. Two potential explanations for the ferroelectricity of Lys@C₆₀ crystals are proposed. First, C₆₀ doping may lower the overall symmetry of the Lys@C₆₀ crystal hybrid due to disordered C₆₀ distribution, enabling switchable spontaneous polarization. Second, C₆₀ doping might enhance the conductivity of Lys@C₆₀ crystals, influencing the electric charge distribution and changing spontaneous polarization, resulting in ferroelectricity. The detailed mechanism warrants further exploration. In summary, with their natural biocompatibility and newfound ferroelectric effect, Lys@C₆₀ crystals present a competitive alternative to traditional piezoelectric energy harvesting systems, especially in biomedical applications where they can be utilized as biodegradable implantable devices like pacemakers and artificial synapses.

5. Conclusions

In summary, we propose a simple C₆₀ doping strategy to endow non-conductive and non-ferroelectric lysozyme crystals with conductive and ferroelectric properties. Our methodology involves enhancing the stability and electroding of Lys@C₆₀ crystals for electric-mechanical measurements. Results from c-AFM and SS-PMF analyses demonstrate that C₆₀ doping endows ferroelectricity and conductivity to tetragonal lysozyme crystals. The increased conductivity of Lys@C₆₀ crystals is attributed to the disorderly arrangement of C₆₀ within the lysozyme crystal, forming specific hole-electron pairs capable of carrying current under an electric field. Additionally, the enhanced conductivity and reduced symmetry contribute to the ferroelectricity of Lys@C₆₀ crystals. Therefore, this work verifies that C₆₀ doping can serve as a simple yet effective strategy to impart novel ferroelectric properties to lysozyme crystals, potentially rendering them suitable for energy storage

and conversion to achieve biocompatible and biodegradable implantable and wearable bioelectronics applications.

Supplementary Materials: The following supporting information can be downloaded at: <https://www.mdpi.com/article/10.3390/cryst14040339/s1>, Figure S1: The physical properties of 32 point groups categorized depending on their symmetry; Figure S2: The diffraction spectra of lysozyme crystal; Figure S3: Cell viability of HEK 293 cells treated with various concentration of Lys@C60; Figure S4: Electroding of Lys@C60 crystals. (a) the ITO electrode with Lys@C60 crystals; (b) the Ni foam electrode with Lys@C60 crystals; Figure S5: The electrical properties of Lys@C60 crystals growth on Ni foam. (a) the EIS of Lys@C60 crystals; (b) the I-T curve of Lys@C60 crystals; Table S1: The diffraction data of Lys@C60 crystal and lysozyme crystals.

Author Contributions: Methodology, R.Z., X.L., W.G. and D.Y.; Software, W.G.; Validation, R.Z. and D.Y.; Formal analysis, X.L.; Investigation, R.Z.; Resources, D.Y.; Data curation, X.L.; Writing—original draft, R.Z.; Writing—review & editing, D.Y.; Visualization, R.Z.; Supervision, D.Y.; Project administration, D.Y.; Funding acquisition, D.Y. All authors have read and agreed to the published version of the manuscript.

Funding: This work was supported by the National Natural Science Foundation of China (NSFC) (Grant No. 82172063), the Science and Technology Program of Ali Region, Tibet (Program No. QYXTZX-AL2022-07), Key R&D Project in Shaanxi Province (Grant No. 2023-YBNI-068), and the Fundamental Research Funds for the Central Universities (Grant No. 23GH02021).

Institutional Review Board Statement: Not applicable.

Informed Consent Statement: Not applicable.

Data Availability Statement: Data are contained within the article.

Conflicts of Interest: The author declares no conflicts of interest.

References

1. Liao, W.-Q.; Zeng, Y.-L.; Tang, Y.-Y.; Peng, H.; Liu, J.-C.; Xiong, R.-G. Multichannel control of multiferroicity in single-component homochiral organic crystals. *J. Am. Chem. Soc.* **2021**, *143*, 21685–21693. [[CrossRef](#)] [[PubMed](#)]
2. Yuan, X.; Shi, J.; Kang, Y.; Dong, J.; Pei, Z.; Ji, X. Piezoelectricity, Pyroelectricity and Ferroelectricity in Biomaterials and Biomedical Applications. *Adv. Mater.* **2023**, *36*, 2308726. [[CrossRef](#)] [[PubMed](#)]
3. Guerin, S.; Stapleton, A.; Chovan, D.; Mouras, R.; Gleeson, M.; McKeown, C.; Noor, M.R.; Silien, C.; Rhen, F.M.F.; Kholkin, A.L.; et al. Control of piezoelectricity in amino acids by supramolecular packing. *Nat. Mater.* **2018**, *17*, 180–186. [[CrossRef](#)] [[PubMed](#)]
4. Panda, S.; Hajra, S.; Song, H.; Jo, J.; Kim, N.; Hwang, S.; Choi, Y.; Kim, H.G.; Kim, H.J.; Mishra, Y.K. Pyroelectric based energy harvesting devices: Hybrid structures and applications. *Sustain. Energy Fuels* **2023**, *7*, 5319–5335. [[CrossRef](#)]
5. Hu, P.; Hu, S.; Huang, Y.; Reimers, J.R.; Rappe, A.M.; Li, Y.; Stroppa, A.; Ren, W. Bioferroelectric properties of glycine crystals. *J. Phys. Chem. Lett.* **2019**, *10*, 1319–1324. [[CrossRef](#)] [[PubMed](#)]
6. Yun, Y.; Buragohain, P.; Li, M.; Ahmadi, Z.; Zhang, Y.; Li, X.; Wang, H.; Li, J.; Lu, P.; Tao, L.; et al. Intrinsic ferroelectricity in Y-doped HfO₂ thin films. *Nat. Mater.* **2022**, *21*, 903–909. [[CrossRef](#)] [[PubMed](#)]
7. Sirotnin, Y.I.; Shaskol'skaia, M.P. *Fundamentals of Crystal Physics*; MIR Publishers: Moscow, Russia, 1982.
8. Stapleton, A.; Noor, M.R.; Sweeney, J.; Casey, V.; Kholkin, A.L.; Silien, C.; Gandhi, A.A.; Soulmane, T.; Tofail, S.A.M. The direct piezoelectric effect in the globular protein lysozyme. *Appl. Phys. Lett.* **2017**, *111*, 142902. [[CrossRef](#)]
9. Lee, D.H.; Lee, Y.; Cho, Y.H.; Choi, H.; Kim, S.H.; Park, M.H. Unveiled Ferroelectricity in Well-Known Non-Ferroelectric Materials and Their Semiconductor Applications. *Adv. Funct. Mater.* **2023**, *33*, 2303956. [[CrossRef](#)]
10. Kim, K.-H.; Ko, D.-K.; Kim, N.H.; Paul, J.; Zhang, S.-Q.; Murray, C.B.; Acharya, R.; DeGrado, W.F.; Kim, Y.H.; Grigoryan, G. Protein-directed self-assembly of a fullerene crystal. *Nat. Commun.* **2016**, *7*, 11429. [[CrossRef](#)]
11. Minary-Jolandan, M.; Yu, M.-F. Uncovering nanoscale electromechanical heterogeneity in the subfibrillar structure of collagen fibrils responsible for the piezoelectricity of bone. *ACS Nano* **2009**, *3*, 1859–1863. [[CrossRef](#)]
12. Harnagea, C.; Vallières, M.; Pfeiffer, C.P.; Wu, D.; Olsen, B.R.; Pignolet, A.; Légaré, F.; Gruverman, A. Two-dimensional nanoscale structural and functional imaging in individual collagen type I fibrils. *Biophys. J.* **2010**, *98*, 3070–3077. [[CrossRef](#)] [[PubMed](#)]
13. Minary-Jolandan, M.; Yu, M.-F. Nanoscale characterization of isolated individual type I collagen fibrils: Polarization and piezoelectricity. *Nanotechnology* **2009**, *20*, 085706. [[CrossRef](#)] [[PubMed](#)]
14. Liu, Y.; Cai, H.-L.; Zelisko, M.; Wang, Y.; Sun, J.; Yan, F.; Ma, F.; Wang, P.; Chen, Q.C.; Zheng, H.; et al. Ferroelectric switching of elastin. *Proc. Natl. Acad. Sci. USA* **2014**, *111*, E2780–E2786. [[CrossRef](#)] [[PubMed](#)]
15. Liu, Y.; Wang, Y.; Chow, M.-J.; Chen, N.Q.; Ma, F.; Zhang, Y.; Li, J. Glucose suppresses biological ferroelectricity in aortic elastin. *Phys. Rev. Lett.* **2013**, *110*, 168101. [[CrossRef](#)] [[PubMed](#)]

16. Stapleton, A.; Ivanov, M.S.; Noor, M.R.; Silien, C.; Gandhi, A.A.; Soulimane, T. Converse piezoelectricity and ferroelectricity in crystals of lysozyme protein revealed by piezoresponse force microscopy. *Ferroelectrics* **2018**, *525*, 135–145. [[CrossRef](#)]
17. Denning, D.; Kilpatrick, J.L.; Fukada, E.; Zhang, N.; Habelitz, S.; Fertala, A.; Gilchrist, M.D.; Zhang, Y.; Tofail, S.A.M.; Rodriguez, B.J. Piezoelectric tensor of collagen fibrils determined at the nanoscale. *ACS Biomater. Sci. Eng.* **2017**, *3*, 929–935. [[CrossRef](#)] [[PubMed](#)]
18. Miao, L.-P.; Ding, N.; Wang, N.; Shi, C.; Ye, H.-Y.; Li, L.; Yao, Y.-F.; Dong, S.; Zhang, Y. Direct observation of geometric and sliding ferroelectricity in an amphidynamic crystal. *Nat. Mater.* **2022**, *21*, 1158–1164. [[CrossRef](#)] [[PubMed](#)]
19. Soldà, A.; Cantelli, A.; Di Giosia, M.; Montalti, M.; Zerbetto, F.; Rapino, S.; Calvaresi, M. C 60@ lysozyme: A new photosensitizing agent for photodynamic therapy. *J. Mater. Chem. B* **2017**, *5*, 6608–6615. [[CrossRef](#)] [[PubMed](#)]
20. Brahmkhatri, V.; Atreya, H.S. Dynamics of Protein–Nanoparticle Interactions Using NMR. In *NMR Spectroscopy for Probing Functional Dynamics at Biological Interfaces*; Royal Society of Chemistry: London, UK, 2022; pp. 236–253.
21. Zhou, R.; Ohulchanskyy, T.Y.; Xu, Y.; Ziniuk, R.; Xu, H.; Liu, L.; Qu, J. Tumor-microenvironment-activated NIR-II nanotheranostic platform for precise diagnosis and treatment of colon cancer. *ACS Appl. Mater. Interfaces* **2022**, *14*, 23206–23218. [[CrossRef](#)]
22. Zhou, R.; Xu, H.; Qu, J.; Ohulchanskyy, T.Y. Hemoglobin nanocrystals for drugs free, synergistic theranostics of colon tumor. *Small* **2023**, *19*, 2205165. [[CrossRef](#)]
23. Afonine, P.V.; Grosse-Kunstleve, R.W.; Echols, N.; Headd, J.J.; Moriarty, N.W.; Mustyakimov, M.; Terwilliger, T.C.; Urzhumtsev, A.; Zwart, P.H.; Adams, P.D. Towards automated crystallographic structure refinement with phenix.refine. *Acta Crystallogr. Sect. D Biol. Crystallogr.* **2012**, *68*, 352–367. [[CrossRef](#)]
24. Emsley, P.; Cowtan, K. Coot: Model-building tools for molecular graphics. *Acta Crystallogr. Sect. D Biol. Crystallogr.* **2004**, *60*, 2126–2132. [[CrossRef](#)]
25. Murshudov, G.N.; Vagin, A.A.; Dodson, E.J. Refinement of macromolecular structures by the maximum-likelihood method. *Acta Crystallogr. Sect. D Biol. Crystallogr.* **1997**, *53*, 240–255. [[CrossRef](#)] [[PubMed](#)]
26. Lanza, M. *Conductive Atomic Force Microscopy: Applications in Nanomaterials*; John Wiley & Sons: Hoboken, NJ, USA, 2017.
27. Jesse, S.; Baddorf, A.P.; Kalinin, S.V. Switching spectroscopy piezoresponse force microscopy of ferroelectric materials. *Appl. Phys. Lett.* **2006**, *88*, 062908. [[CrossRef](#)]
28. Liu, H.-Y.; Zhang, H.-Y.; Chen, X.-G.; Xiong, R.-G. Molecular design principles for ferroelectrics: Ferroelectrochemistry. *J. Am. Chem. Soc.* **2020**, *142*, 15205–15218. [[CrossRef](#)] [[PubMed](#)]
29. Tang, X.H.; Liu, J.J.; Zhang, Y.; Wang, X.Z. Study on the influence of lysozyme crystallization conditions on crystal properties in crystallizers of varied sizes when temperature is the manipulated variable. *J. Cryst. Growth* **2018**, *498*, 186–196. [[CrossRef](#)]
30. Shi, P.-P.; Tang, Y.-Y.; Li, P.-F.; Liao, W.-Q.; Wang, Z.-X.; Ye, Q.; Xiong, R.-G. Symmetry breaking in molecular ferroelectrics. *Chem. Soc. Rev.* **2016**, *45*, 3811–3827. [[CrossRef](#)]
31. Tait, S.L.; White, E.T.; Litster, J.D. Mechanical characterization of protein crystals. *Part. Part. Syst. Charact.* **2008**, *25*, 266–276. [[CrossRef](#)]
32. Zhou, R.; Ohulchanskyy, T.Y.; Xu, H.; Ziniuk, R.; Qu, J. Catalase Nanocrystals Loaded with Methylene Blue as Oxygen Self-Supplied, Imaging-Guided Platform for Photodynamic Therapy of Hypoxic Tumors. *Small* **2021**, *17*, 2103569. [[CrossRef](#)] [[PubMed](#)]
33. Bonnell, D.; Kalinin, S.; Kholkin, A.; Gruverman, A. Piezoresponse force microscopy: A window into electromechanical behavior at the nanoscale. *MRS Bull.* **2009**, *34*, 648–657. [[CrossRef](#)]
34. Wang, W.; Li, J.; Liu, H.; Ge, S. Advancing versatile ferroelectric materials toward biomedical applications. *Adv. Sci.* **2021**, *8*, 2003074. [[CrossRef](#)] [[PubMed](#)]

Disclaimer/Publisher’s Note: The statements, opinions and data contained in all publications are solely those of the individual author(s) and contributor(s) and not of MDPI and/or the editor(s). MDPI and/or the editor(s) disclaim responsibility for any injury to people or property resulting from any ideas, methods, instructions or products referred to in the content.